

## Article

# The Effect of Deposition Parameters on Morphological and Optical Properties of Cu<sub>2</sub>S Thin Films Grown by Chemical Bath Deposition Technique

Honar S. Ahmed  and Raghad Y. Mohammed \* 

Department of Physics, College of Science, University of Duhok, Duhok 42001, Kurdistan Region, Iraq; honar.salah@uod.ac

\* Correspondence: ssraghad@uod.ac

**Abstract:** The chemical bath deposition technique has been used for the deposition of Cu<sub>2</sub>S thin films on glass substrates. The thickness of deposited thin films strongly depends on the deposition parameters. The present study revealed that the thickness increased from 185 to 281 nm as deposition time increased and from 183 to 291 nm as bath temperature increased. In addition, the thickness increased from 257 to 303 nm with the increment of precursors concentration and from 185 to 297 nm as the pH value increased. However, the thickness decreased from 299 to 234 nm with the increment of precursors concentration. The morphology of Cu<sub>2</sub>S thin films remarkably changed as the deposition parameters varied. The increase in deposition time, bath temperature, and CuSO<sub>4</sub>·5H<sub>2</sub>O concentration leads to the increase in particle sizes, homogeneity, compactness of the thin films, and the number of clusters, and agglomeration, while the increase in thiourea concentration leads to the decrease in particle sizes and quality of films. Optical results demonstrated that the transmission of thin films rapidly increased in the UV–VIS region at ( $\lambda = 350\text{--}500\text{ nm}$ ) until it reached its maximum peak at ( $\lambda = 600\text{--}650\text{ nm}$ ) in the visible region, then it decreased in the NIR region. The high absorption was obtained in the UV–VIS region at ( $\lambda = 350\text{--}500\text{ nm}$ ) before it decreased to its minimum value in the visible region, and then increased in the NIR region. The energy bandgap of thin films effectively depends on the deposition parameters. It decreased with the increasing deposition time (3.01–2.95 eV), bath temperature (3.04–2.63 eV), CuSO<sub>4</sub>·5H<sub>2</sub>O concentration (3.1–2.6 eV), and pH value (3.14–2.75 eV), except for thiourea concentration, while it decreased with the increasing thiourea concentration (2.79–3.09 eV).

**Keywords:** Cu<sub>2</sub>S thin film; chemical bath deposition; energy bandgap; thin films; optical properties; thickness measurements; deposition parameters



**Citation:** Ahmed, H.S.; Mohammed, R.Y. The Effect of Deposition Parameters on Morphological and Optical Properties of Cu<sub>2</sub>S Thin Films Grown by Chemical Bath Deposition Technique. *Photonics* **2022**, *9*, 161. <https://doi.org/10.3390/photonics9030161>

Received: 17 January 2022

Accepted: 4 March 2022

Published: 6 March 2022

**Publisher's Note:** MDPI stays neutral with regard to jurisdictional claims in published maps and institutional affiliations.



**Copyright:** © 2022 by the authors. Licensee MDPI, Basel, Switzerland. This article is an open access article distributed under the terms and conditions of the Creative Commons Attribution (CC BY) license (<https://creativecommons.org/licenses/by/4.0/>).

## 1. Introduction

Transition metal chalcogenides have been attracting great interest due to their physical and chemical properties. These properties are beneficial in various applications, such as optical sensors, solar energy conversion, sensors for low temperatures, catalysts, and microelectronic devices [1–5]. The copper sulfide (Cu<sub>x</sub>S) system has five different phases, including chalcocite, djurleite, digenite, anilite, and covellite. Additionally, it depends on the value of  $X = 2, 1.95, 1.8, 1.75, \text{ and } 1$ , respectively [6–9]. Bulk Cu<sub>2</sub>S solids are classified as  $\alpha$  phase (stable above 425 °C),  $\beta$  phase (high chalcocite; stable between 105 and 425 °C), and  $\gamma$  phase (low chalcocite; the first solid–liquid hybrid phase and stable below 105 °C) [10,11].

Cu<sub>2</sub>S has crucial properties, such as non-toxicity, low cost [12], and an ideal bandgap. In addition, it plays an important role in various applications, including solar energy absorbers [13], electroconductive coatings [14], tabular solar collectors [15], ion batteries and superconductors [16,17], heterojunction photodetectors, such as Cu<sub>2</sub>S/CdS, ZnO/Cu<sub>2</sub>S, Cu<sub>2</sub>S/ZnS, and Cu<sub>2</sub>S/n-Si [18–20], and sensors [3]. Various deposition techniques are

utilized for the synthetization of  $\text{Cu}_2\text{S}$  thin films, such as vacuum evaporation [21], photochemical deposition [22], chemical bath deposition [15,23,24], sputtering [25], continuous flow microreactor [26,27], spray pyrolysis [28,29], and successive ionic layer adsorption and reaction technique (SILAR) [30,31]. The chemical bath deposition technique is one of the most popular techniques for the deposition of thin films due to its advantage over other deposition techniques, such as low cost, low pressure, ability to deposit large areas, and low-temperature requirement [15,32,33]. The properties of chemically deposited thin films strongly depend on the deposition parameters, such as deposition time [23], pH value [34,35], bath temperature [36], and substrate nature [13,33,37].

In the present study, the chemical bath deposition technique has been utilized for the synthetization of  $\text{Cu}_2\text{S}$  thin films. The growth, morphological, structural, and optical properties of deposited thin films have been studied as a function of deposition parameters (deposition time ( $t_d$ ), bath temperature ( $T_b$ ), pH value, precursors concentration (copper sulfate pentahydrate ( $\text{CuSO}_4 \cdot 5\text{H}_2\text{O}$ ), and thiourea concentration ( $\text{SC}(\text{NH}_2)_2$ )).

## 2. Experiment

### 2.1. Cleaning Process

Glass substrates with dimensions of  $25 \times 75 \times 1$  mm have been immersed in chromic acid for 24 h. Then, the substrates were ultrasonically cleaned with distilled water and rinsed in ethanol. Thereafter, they were maintained inside a desiccator to deposit  $\text{Cu}_2\text{S}$  thin films.

### 2.2. Deposition of $\text{Cu}_2\text{S}$ Thin Films

Initially, the  $\text{CuSO}_4 \cdot 5\text{H}_2\text{O}$  precursor was used as a source of  $\text{Cu}^+$  ions by diluting the solution in 50 mL of distilled water. Under continuous stirring, 2 mL of triethanolamine (TEA;  $\text{C}_6\text{H}_{15}\text{NO}_3$ ) acted as a complex agent. Then, 15% of ammonia solution was consecutively added to achieve the desired pH value. Subsequently, the color of the solution changed to dark blue, which indicates the formation of copper ions. Then, 50 mL of thiourea ( $\text{SC}(\text{NH}_2)_2$ ) solution as a source of  $\text{S}^-$  was added to the solution. The color of the solution changed from dark blue to dark brown during the deposition process, which indicates the steps of the formation of  $\text{Cu}_2\text{S}$  thin films, as shown in Figure 1. The reactions inside the bath can be expressed as shown in Equations (1) and (2) [36]. Thereafter, the substrate was immersed vertically in the solution. The deposition process was carried out at various deposition parameters and presented in Table 1.

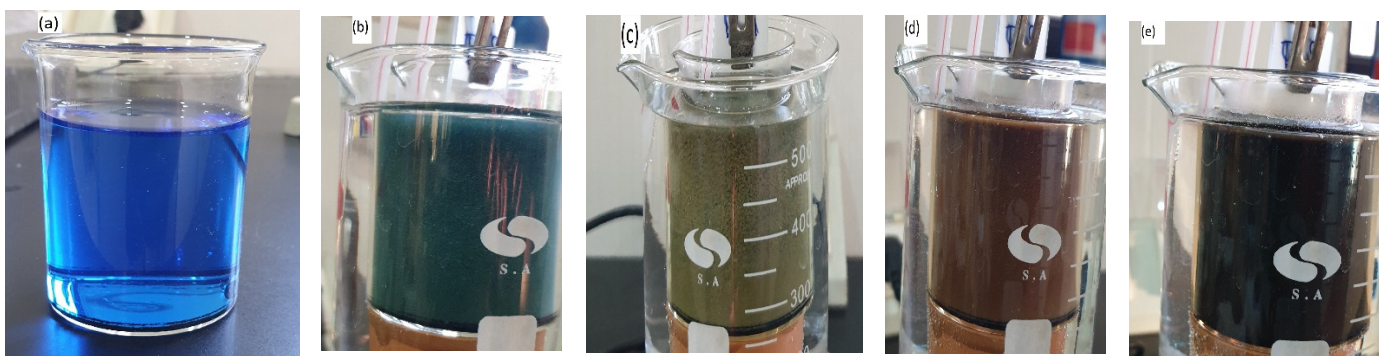
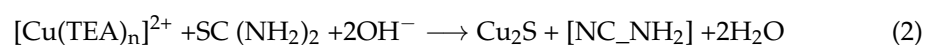


**Figure 1.** The stages of chemical bath deposition of  $\text{Cu}_2\text{S}$ : (a) 0 min, (b) after 2 min, (c) 3 min, (d) 5 min, and (e) 6.5 min with  $\text{CuSO}_4 \cdot 5\text{H}_2\text{O} = 3$  M,  $\text{SC}(\text{NH}_2)_2 = 1$  M, bath temperature =  $70^\circ\text{C}$ , and  $\text{pH} = 10$ .

**Table 1.** Chemical bath solutions.

| Bath No. | t (min)     | CuSO <sub>4</sub> ·5H <sub>2</sub> O (M) | SC (NH <sub>2</sub> ) <sub>2</sub> (M) | T (°C)                 | pH Value     | TEA (mL) |
|----------|-------------|--|--|------------------------|--------------|----------|
| 1        | 2–10 step 2 | 0.3                                      | 1                                      | 70                     | 10           | 2        |
| 2        | 8           | 0.1, 0.5                                 | 1                                      | 70                     | 10           | 2        |
| 3        | 8           | 0.3                                      | 0.4–1.2 step 0.2                       | 70                     | 10           | 2        |
| 4        | 8           | 0.3                                      | 1                                      | 70                     | 8, 9, and 11 | 2        |
| 5        | 8           | 0.3                                      | 1                                      | 40, 50, 60, 80, and 90 | 10           | 2        |

The thickness of Cu<sub>2</sub>S was measured using an optical interferometer technique [38–40]:

$$d = \frac{\Delta x}{x} \frac{\lambda}{2} \tag{3}$$

where *d* is the thin film thickness, He–Ne is the laser wavelength ( $\lambda = 632.8$  nm),  $\Delta x$  is the distance between two fringes, and *x* is the width of the fringe.

### 2.3. Characterization of Cu<sub>2</sub>S Thin Films

The morphological properties of Cu<sub>2</sub>S thin films has been studied by the MIRA 3 TESCAN scanning electron microscopy (SEM). The optical transmission measurements of Cu<sub>2</sub>S thin films were obtained using an UV–Vis spectrophotometer (JANEWAY 6850) in the range of 350–1100 nm.

The direct energy bandgap of Cu<sub>2</sub>S thin films was calculated using Tauc’s equation:

$$(\alpha h\nu)^2 = B(h\nu - E_g)^n \tag{4}$$

where the bandgap energy (*E<sub>g</sub>*), the transmittance (*T*), the absorption (*A*), and the absorption coefficient ( $\alpha$ ) are given by ( $=2.303 \log (T/d)$ ). In addition, (*hν*) is the incident photon energy, *n* depends on the transition type (which is equal to 1/2 for the allowed direct transition and 2 for the indirect one), and (*d*) is the film thickness [41,42].

## 3. Results and Discussion

### 3.1. Deposition Parameters

Figure 2 presents the thickness and growth rate variation of Cu<sub>2</sub>S thin films as a function of deposition parameters (deposition time, bath temperature, CuSO<sub>4</sub>·5H<sub>2</sub>O concentration, pH value, and SC (NH<sub>2</sub>)<sub>2</sub> concentration).

In Figure 2a, the thickness of deposited thin films increased almost linearly as deposition time increased from 2 to 6 min. Thereafter, the thickness started to decrease when the time reached 8 min, with a significant decrease at deposition time of 10 min. This decrement can be attributed to the porous formation of an outer layer and peeling off from the glass substrate [43]. The growth rate of deposited films (Figure 2a) gradually decreased with the deposition time, which can be attributed to the precursor consumption over time [42].

The thickness increased as bath temperature increased, until it reached its saturation point at a bath temperature of 70 °C. Thereafter, when the temperature reached 80 °C, the thickness started to decrease due to the desorption and/or dissolution of preformed Cu<sub>2</sub>S [44], as shown in Figure 2b. While the growth rate of deposited films gradually increased with the bath temperature due to additional generations of colloidal ions [42], as shown in Figure 2b.

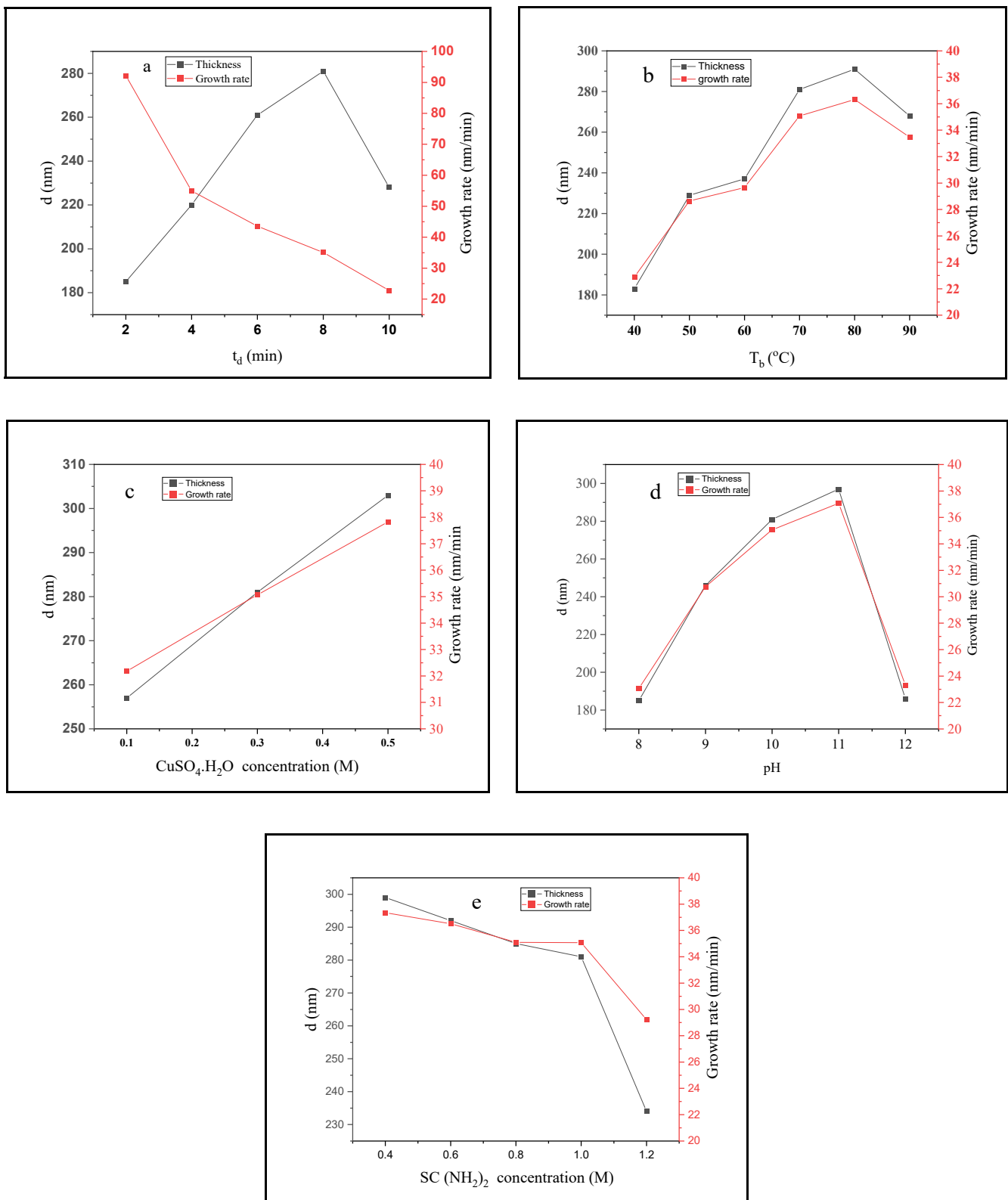


**Figure 2.** The thickness and growth rate variation of  $\text{Cu}_2\text{S}$  thin films as a function of deposition parameters: (a) Deposition time, (b) bath temperature, (c)  $\text{CuSO}_4 \cdot 5\text{H}_2\text{O}$  concentration, (d) pH value, (e) and  $\text{SC}(\text{NH}_2)_2$  concentration.

In Figure 2c, the thickness and growth rate increased as  $\text{CuSO}_4 \cdot 5\text{H}_2\text{O}$  concentration increased. This is attributed to the competition of heterogeneous nucleation on the substrate and homogeneous nucleation in the solution, which could modify the growth of thin films and increase the thickness [45].

The thickness of  $\text{Cu}_2\text{S}$  thin films almost linearly increased from 185 to 297 nm as the pH value of bath solution increased from 8 to 11, as shown in Figure 2d.

This increase in thickness is attributed to the increment of  $\text{OH}^-$  ions concentration in the solution that pushes the reaction of thiourea hydrolysis forward, causing the high generation of sulfide ions [46], as shown in Figure 2d. In addition, the growth rate increased as the pH value increased (Figure 2d).

Figure 2e shows the effect of SC  $(\text{NH}_2)_2$  concentration on the thickness of deposited thin films.

Notably, the thickness of deposited thin films decreased as the SC  $(\text{NH}_2)_2$  concentration increased due to the limited concentration of  $\text{Cu}^{2+}$  and  $\text{S}^{2-}$  ions that was released in the solution [39]. The growth rate of  $\text{Cu}_2\text{S}$  thin films can be seen in Figure 2e.

### 3.2. Physical Properties

#### 3.2.1. Morphological Properties

Figure 3 demonstrated the SEM images of  $\text{Cu}_2\text{S}$  thin films at various deposition parameters (deposition time, bath temperature, pH value,  $\text{CuSO}_4 \cdot 5\text{H}_2\text{O}$  concentration, and SC  $(\text{NH}_2)_2$  concentration).

Figure 3a shows that the FESEM images of thin films at deposition time of 6 min were uniform, well covered, and homogenous without cracks. In addition, the increase in deposition time leads to the increase in aggregations. Moreover, few cracks were found in both deposited thin films at 8 and 10 min. The number and size of the grain increased from 37.25 to 99.57 nm as deposition time increased from 6 to 10 min. Figure 3a indicates that additional nucleation sites have formed [47]. The increase in bath temperature leads to the increase in compactness, homogeneity, and uniformity of films, as shown in Figure 3b. The surface of films deposited at 40 °C was not completely covered and had few cracks. However, the surface of films deposited at 70 and 90 °C was homogeneous, compact, and relatively completely covered and uniform.

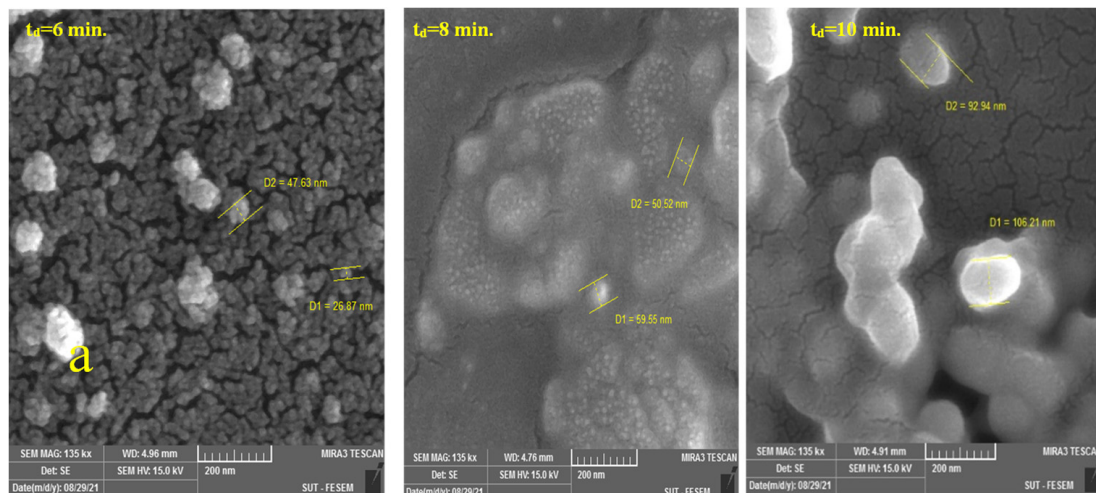


Figure 3. Cont.

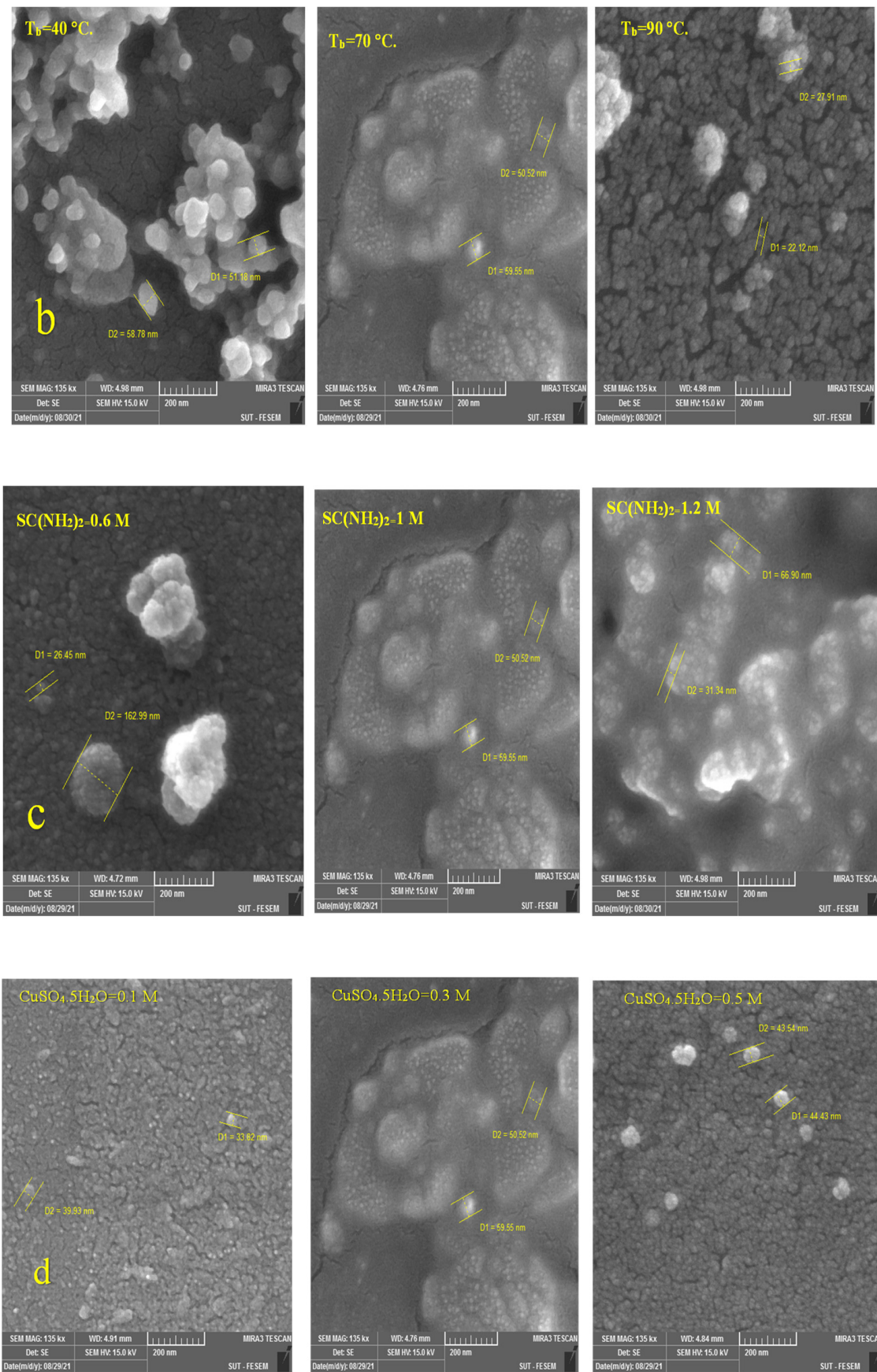
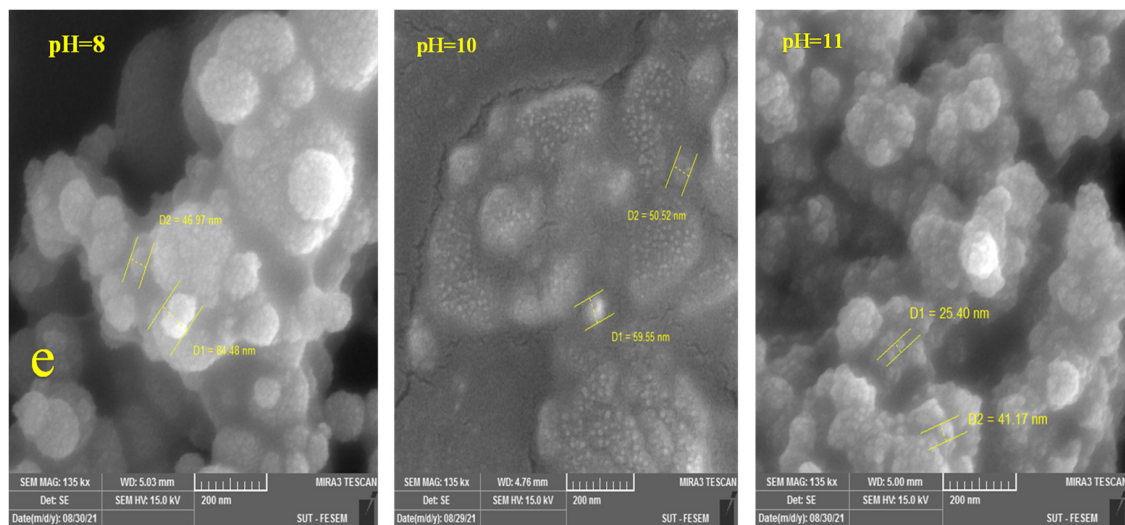


Figure 3. Cont.



**Figure 3.** FESEM images of  $\text{Cu}_2\text{S}$  thin films at different deposition parameters: (a) Deposition time ( $t_d$ ), (b) bath temperature ( $T_b$ ), (c)  $\text{SC}(\text{NH}_2)_2$  concentration, (d)  $\text{CuSO}_4 \cdot 5\text{H}_2\text{O}$  concentration, and (e) pH value.

The deposited films at 0.6 and 1 M of  $\text{SC}(\text{NH}_2)_2$  concentration are well covered, uniform, and homogeneous with few small cracks on the surface deposited at 1 M of  $\text{SC}(\text{NH}_2)_2$  concentration. The quality of thin films decreased as the  $\text{SC}(\text{NH}_2)_2$  concentration increased to 1.2 M. Agglomerations and cracks existed on the film's surface, as shown in Figure 3c. Deposited thin films at various  $\text{CuSO}_4 \cdot 5\text{H}_2\text{O}$  molar concentrations were well covered, uniform, homogeneous, and few small cracks existed on the surface of the films deposited at 0.3 and 0.5 M, as shown in Figure 3d. However, the average particle sizes were 36.87, 55.03, and 43.98 nm for the deposited thin films at 0.1, 0.3, and 0.5 M of  $\text{CuSO}_4 \cdot 5\text{H}_2\text{O}$  molar concentration, respectively. The increase in  $\text{CuSO}_4 \cdot 5\text{H}_2\text{O}$  molar concentration leads to the increase in the number of clusters and agglomerated nanoparticles. The FESEM images of deposited films at different pH values are shown in Figure 3e. The films were homogeneous and well covered. However, the agglomerations and clusters increased as the pH value increased. The average particle sizes decreased from 65.72 to 33.28 nm as the pH value increased from 8 to 11. The increase in the pH value leads to noticeable changes in the morphology of deposited thin films due to the increment of  $\text{OH}^-$  ions. This leads the reaction forward, increase the attractive force and decrease repulsive force, which allow for the growth of oriented attachment (OA). When the particles are perfectly aligned, the common boundary is eliminated, resulting in the formation of larger well-defined morphology particles [48,49].

### 3.2.2. Optical Properties

Figure 4 shows the transmission of  $\text{Cu}_2\text{S}$  thin films deposited at different deposition parameters (deposition time, bath temperature,  $\text{CuSO}_4 \cdot 5\text{H}_2\text{O}$  concentration,  $\text{SC}(\text{NH}_2)_2$  concentration, and pH value). Notably, the transmittance decreased as these parameters increased. However, the transmittance increased as the  $\text{SC}(\text{NH}_2)_2$  concentration increased. In addition, the transmittance of deposited thin films in the UV–Vis region rapidly increased until it reached its maximum peak at ( $\lambda = 600\text{--}650\text{ nm}$ ). Thereafter, a slight decrease was found in the visible part before the rapid decrease in the NIR region, except for thin films deposited at ( $T_B = 40\text{ }^\circ\text{C}$ ) and ( $\text{pH} = 8$ ), which have high transmittance of 94% and 86.2% at the NIR region. This decrease in transmission is due to the increase in the thickness of deposited  $\text{Cu}_2\text{S}$  thin films [23].

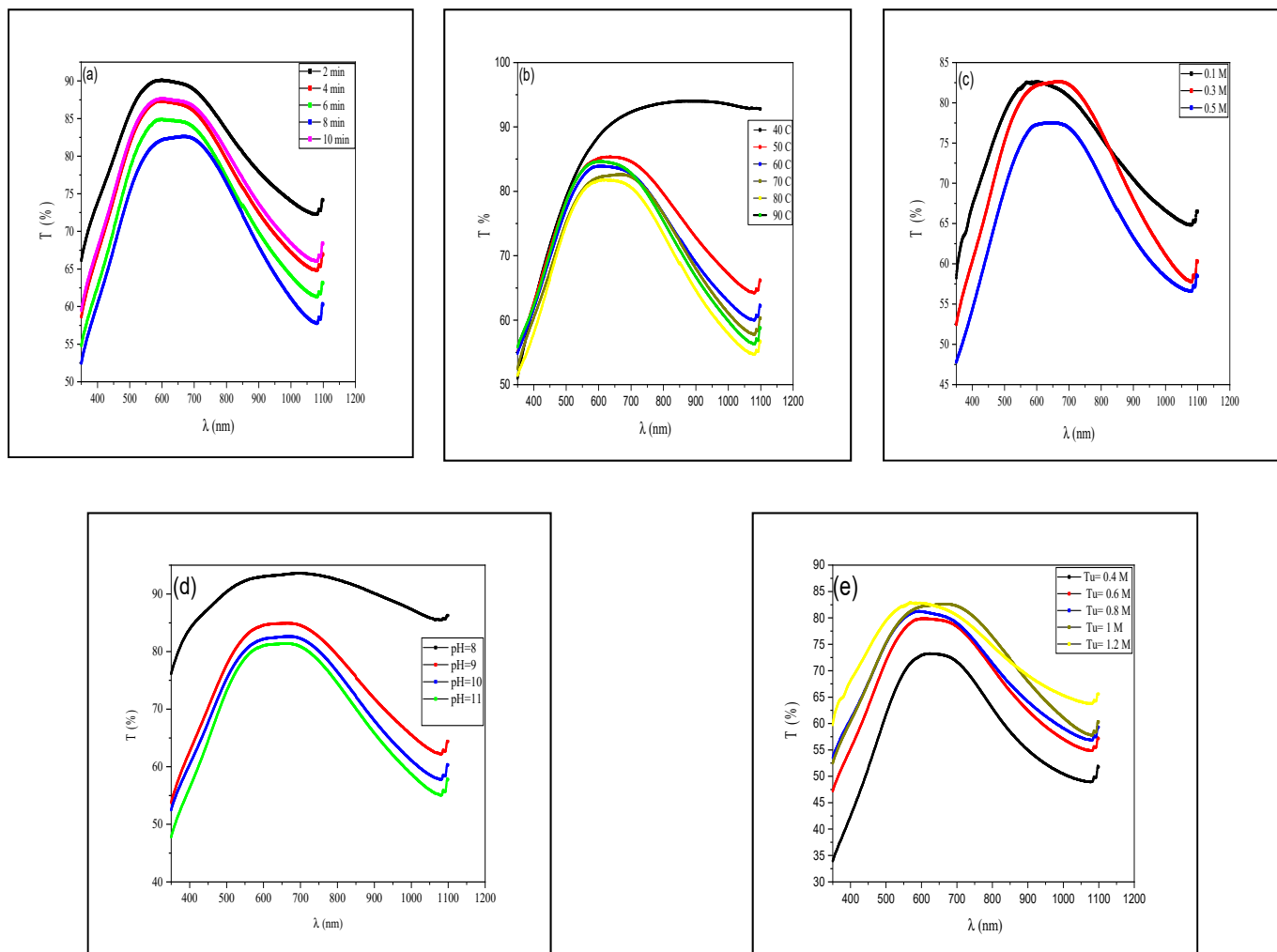


**Figure 4.** Transmission spectra of Cu<sub>2</sub>S thin films as a function of different deposition parameters: (a) Deposition time, (b) bath temperature, (c) CuSO<sub>4</sub>·5H<sub>2</sub>O concentration, (d) pH value, and (e) SC (NH<sub>2</sub>)<sub>2</sub> concentration.

Figure 5 shows the absorbance spectra of Cu<sub>2</sub>S thin films deposited at different deposition parameters. The absorbance of deposited thin films increased as deposition time, bath temperature, CuSO<sub>4</sub>·5H<sub>2</sub>O concentration, and pH value increased. In contrast, it decreased when the SC (NH<sub>2</sub>)<sub>2</sub> concentration increased. In general, all of the deposited thin films have high absorbance at UV and NIR regions, except for thin films deposited at (T<sub>b</sub> = 40 °C) and (pH = 8), which had low absorbance at the NIR region. In addition, thin films had low absorbance at the VIS region. Low transparency in UV region provides thin films with a coating quality for use in eyeglasses to protect the eye from UV radiation [23].

The high absorption coefficient indicates that deposited Cu<sub>2</sub>S thin films with various deposition parameters have a direct energy bandgap [19]. This was calculated from the extrapolation straight-line portion of the curve  $(\alpha h\nu)^2$  versus photon energy, as shown in Figure 6.

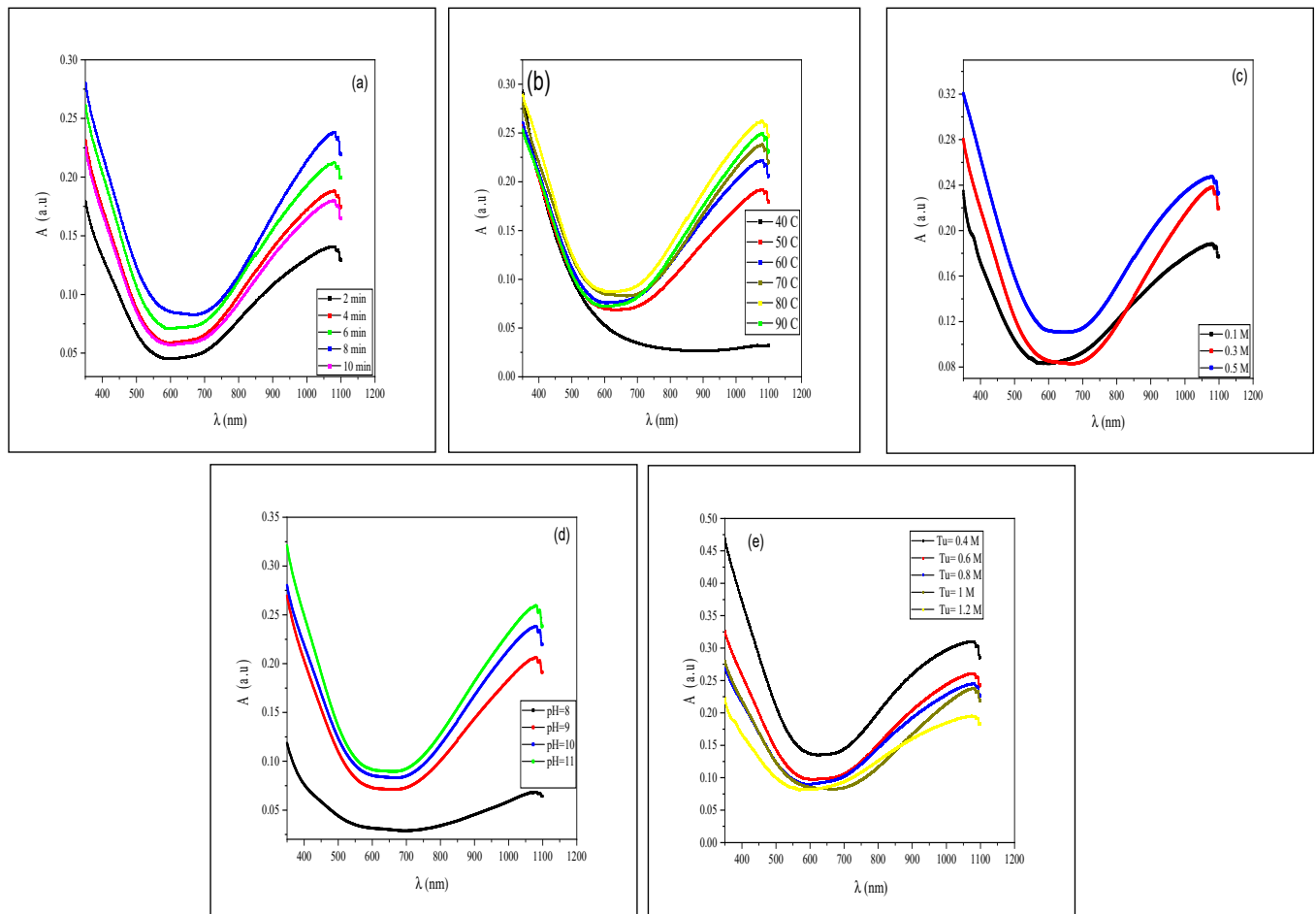


**Figure 5.** Absorbance of  $\text{Cu}_2\text{S}$  thin films as a function of different deposition parameters: (a) Deposition time, (b) bath temperature, (c)  $\text{CuSO}_4 \cdot 5\text{H}_2\text{O}$  concentration, (d) pH value, and (e) SC  $(\text{NH}_2)_2$  concentration.

In Figure 6a and Table 2, the energy gap of deposited thin films decreased as deposition time increased due to the increase in thin films' thickness [19] and crystallinity in the quantum size effect [43]. The decrease in energy gap with the increment of bath temperature is due to the increase in crystallite size, as shown in Figure 6b. This leads to the increased absorption and causes a shift in optical absorption edge towards longer wavelengths, and then the bandgap decreases [50]. In Figure 6c, the energy gap decreased linearly with the increase in  $\text{CuSO}_4 \cdot 5\text{H}_2\text{O}$  concentration due to the increased grain size and low sulfur ions [24]. The obtained energy gap was slightly larger than the previous report by Ismail R.A. et al., which was prepared by a different precursor ( $\text{CuCl}_2$ ) [24]. The energy gap of thin films prepared at different pH values decreased as the pH value of bath solution increased due to the increase in thickness, as shown in Table 2. The obtained value is almost the same as the value obtained by Ahmed H.S. et al. [51], which was prepared by  $\text{Cu}_2\text{S}$  thin films of a different precursor ( $\text{CuCl}_2 \cdot 2\text{H}_2\text{O}$ ). The effect of thickness on the energy gap could increase due to the height of crystalline films and large density of dislocation [21]. The energy gap increased as the SC  $(\text{NH}_2)_2$  concentration increased due to the higher concentration of  $\text{S}^{2-}$  ions, which leads to a decrease in the thickness of thin films. The obtained values are slightly different from the obtained values by Muhammed A.M. et al. [52], which was prepared by  $\text{Cu}_2\text{S}$  thin films of a different precursor ( $\text{CuCl}_2$ ).

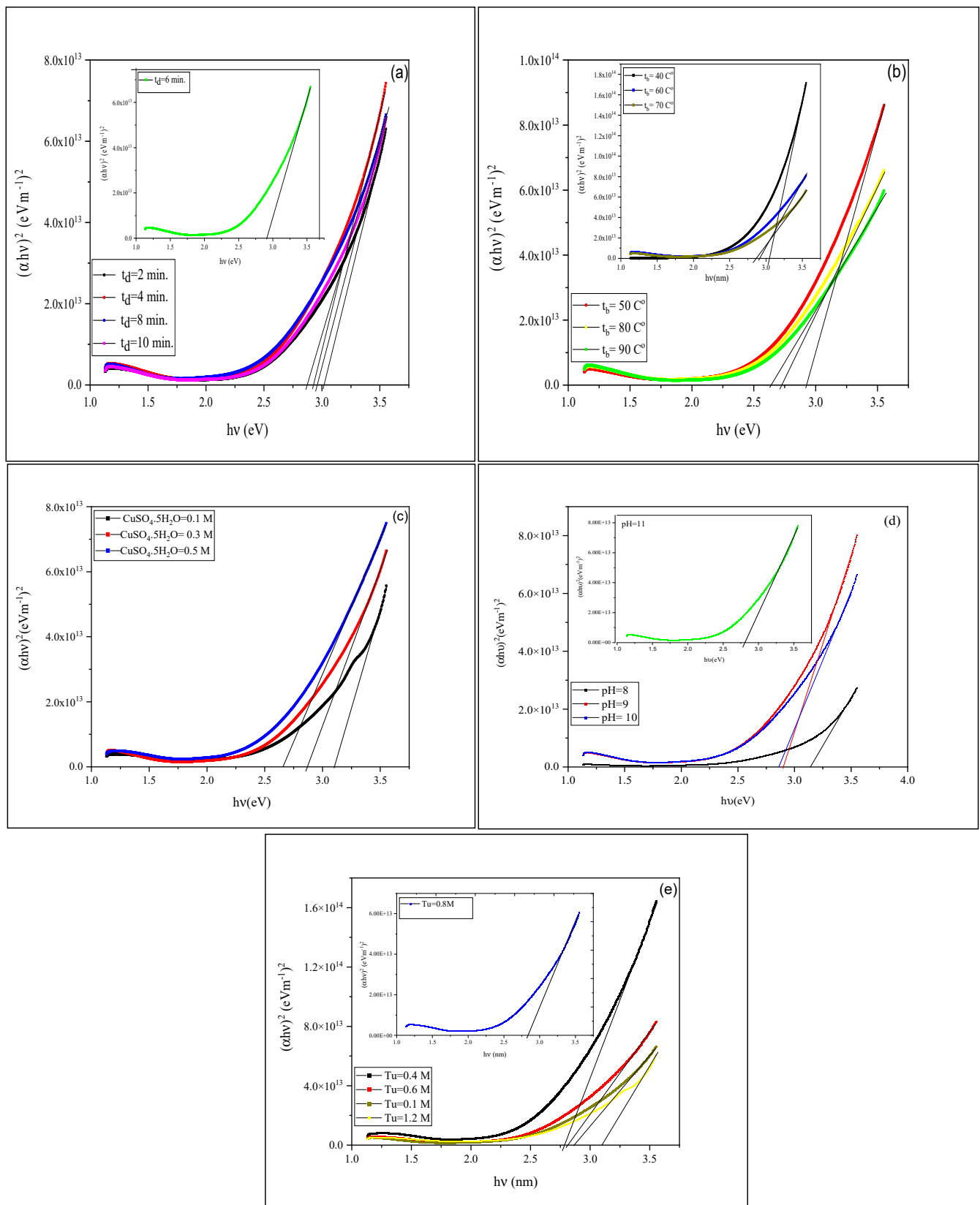


**Figure 6.** Variation of  $(\alpha hv)^2$  with  $(h\nu)$  with deposition parameters): (a) Deposition time, (b) bath temperature, (c)  $\text{CuSO}_4 \cdot 5\text{H}_2\text{O}$  concentration, (d) pH value, and (e) SC ( $\text{NH}_2$ )<sub>2</sub> concentration.

**Table 2.** Bandgap variation with different deposition parameters.

| Bath No.   | 1    | 2    | 3    | 4    | 5    | 6    |
|--|------|------|------|------|------|------|
| Deposition time (min)                                  | 2    | 4    | 6    | 8    | 10   | -    |
| Eg (eV)  | 3.01 | 2.92 | 2.9  | 2.86 | 2.95 | -    |
| Bath temprature (°C)                                   | 40   | 50   | 60   | 70   | 80   | 90   |
| Eg (eV)  | 3.04 | 2.92 | 2.9  | 2.86 | 2.72 | 2.63 |
| CuSO <sub>4</sub> .5H <sub>2</sub> O concentration (M) | 0.1  | 0.3  | 0.5  | -    | -    | -    |
| Eg (eV)  | 3.1  | 2.86 | 2.65 |      |      |      |
| pH Value   | 8    | 9    | 10   | 11   | -    | -    |
| Eg (eV)  | 3.14 | 2.9  | 2.86 | 2.75 |      |      |
| SC (NH <sub>2</sub> ) <sub>2</sub> concentration (M)   | 0.4  | 0.6  | 0.8  | 1    | 1.2  | -    |
| Eg (eV)  | 2.79 | 2.81 | 2.83 | 2.86 | 3.09 | -    |

#### 4. Conclusions

Copper sulfide thin films were successfully deposited by the chemical bath deposition technique. The obtained results indicate that the thickness of deposited thin films strongly depends on the deposition parameters. It increased from 185 to 281 nm as deposition time increased, and from 183 to 291 nm as bath temperature increased. In addition, the thickness increased from 257 to 303 nm as the precursor concentration increased and from 185 to 297 nm as the pH value increased. However, the thickness decreased from 299 to 234 nm with the increasing thiourea concentration. The saturation was found only in the deposition time and bath temperature. The morphology of deposited thin films noticeably changed with the deposition times. The grains' number and size increased with the deposition time. Moreover, the quality improved with the increasing deposition time and decreased at 10 min of deposition time. The deposited Cu<sub>2</sub>S thin films at various CuSO<sub>4</sub>.5H<sub>2</sub>O molar concentrations were compact, uniform, and homogeneous with different particle sizes and clusters, and the agglomerated nanoparticles increased as the CuSO<sub>4</sub>.5H<sub>2</sub>O molar concentration increased. Lower concentrations of thiourea provided compact and homogeneous thin films. The average particle sizes increased as the thiourea concentration increased. The morphology of deposited thin films improved and agglomerated nanoparticles increased as bath temperature increased. The morphology of deposited thin films remarkably changed with the pH value. Deposited thin films at higher pH values were covered almost completely with deposited nanoparticles. The optical measurements demonstrate that almost all of the deposited thin films have high transmission and low absorption in the visible region, while transmittance decreased and absorbance increased in the UV and NIR regions. The energy bandgap of thin films decreased with the increasing deposition time (3.01–2.95 eV), bath temperature (3.04–2.63 eV), CuSO<sub>4</sub>.5H<sub>2</sub>O concentration (3.1–2.6 eV), and pH value (3.14–2.75 eV), except for thiourea concentration, where it decreased with the increase in thiourea concentration (2.79–3.09 eV). Furthermore, all of the deposited thin films have high energy bandgaps and are slightly larger than those obtained by other works.

**Author Contributions:** Conceptualization, R.Y.M.; methodology, R.Y.M. and H.S.A.; software, H.S.A.; validation, R.Y.M. and H.S.A.; formal analysis, R.Y.M. and H.S.A.; investigation, R.Y.M. and H.S.A.; resources, R.Y.M.; data curation, R.Y.M. and H.S.A.; writing—original draft preparation, H.S.A.; writing—review and editing, R.Y.M.; visualization, R.Y.M. and H.S.A.; supervision, R.Y.M.; project administration, R.Y.M. All authors have read and agreed to the published version of the manuscript.

**Funding:** This research received no external funding.

**Institutional Review Board Statement:** Not applicable.

**Informed Consent Statement:** Not applicable.

**Data Availability Statement:** Not applicable.

**Acknowledgments:** The authors are thankful to the University of Duhok for their full support.

**Conflicts of Interest:** The authors declare no conflict of interest.

## References

1. Cruz, J.S.; Hernández, S.M.; Coronel, J. Characterization of  $Cu_xS$  thin films obtained by CBD technique at different annealing temperatures. *Chalcogenide Lett.* **2012**, *9*, 85–91.
2. Munce, C.G. *Chemical Bath Deposition of Copper Sulfide Thin Films*; Griffith University: Queensland, Australia, 2008.
3. Sagade, A.; Sharma, R. Copper sulphide ( $Cu_xS$ ) as an ammonia gas sensor working at room temperature. *Sensors Actuators B Chem.* **2008**, *133*, 135–143. [[CrossRef](#)]
4. Adelifard, M.; Eshghi, H.; Mohagheghi, M.M.B. Comparative studies of spray pyrolysis deposited copper sulfide nanostructural thin films on glass and FTO coated glass. *Bull. Mater. Sci.* **2012**, *35*, 739–744. [[CrossRef](#)]
5. More, P.; Dhanayat, S.; Gattu, K.; Mahajan, S.; Upadhye, D.; Sharma, R. Annealing effect on  $Cu_2S$  thin films prepared by chemical bath deposition. In *AIP Conference Proceedings*; AIP Publishing LLC: Melville, NY, USA, 2016.
6. Dhondge, A.D.; Gosavi, S.R.; Gosavi, N.M.; Sawant, C.P.; Patil, A.M.; Shelke, A.R.; Deshpande, N.G. Influence of Thickness on the Photosensing Properties of Chemically Synthesized Copper Sulfide Thin Films. *World J. Condens. Matter Phys.* **2015**, *05*, 1–9. [[CrossRef](#)]
7. Sabah, F.A.; Ahmed, N.M.; Hassan, Z.; Rasheed, H.S. Effect of Annealing on the Electrical Properties of  $Cu_xS$  Thin Films. *Procedia Chem.* **2016**, *19*, 15–20. [[CrossRef](#)]
8. Bharathi, B.; Thanikaikarasan, S.; Kollu, P.; Chandrasekar, P.V.; Sankaranarayanan, K.; Shajan, S. Effect of substrate on electroplated copper sulphide thin films. *J. Mater. Sci. Mater. Electron.* **2014**, *25*, 5338–5344. [[CrossRef](#)]
9. Naji, I.; Sleman, U. Influence of precursor molar ratios on the physical properties of nanocrystalline  $Cu_{2-x}S$  thin films prepared by chemical bath deposition method. *Chalcogenide Lett.* **2018**, *15*, 317–328.
10. Wang, L.-W. High Chalcocite  $Cu_2S$ : A Solid-Liquid Hybrid Phase. *Phys. Rev. Lett.* **2012**, *108*, 085703. [[CrossRef](#)]
11. Guo, Y.; Wu, Q.; Li, Y.; Lu, N.; Mao, K.; Bai, Y.; Zhao, J.; Wang, J.; Zeng, X.C. Copper (I) sulfide: A two-dimensional semiconductor with superior oxidation resistance and high carrier mobility. *Nanoscale Horiz.* **2019**, *4*, 223–230. [[CrossRef](#)]
12. Hedlund, J.K.; Estrada, T.G.; Walker, A.V. Chemical Bath Deposition of Copper Sulfide on Functionalized SAMs: An Unusual Selectivity Mechanism. *Langmuir* **2020**, *36*, 3119–3126. [[CrossRef](#)]
13. Patil, M.; Sharma, D.; Dive, A.; Mahajan, S.; Sharma, R. Synthesis and Characterization of  $Cu_2S$  Thin Film Deposited by Chemical Bath Deposition Method. *Procedia Manuf.* **2018**, *20*, 505–508. [[CrossRef](#)]
14. Yamamoto, T.; Kubota, E.; Taniguchi, A.; Dev, S.; Tanaka, K.; Osakada, K.; Sumita, M. Electrically conductive metal sulfide-polymer composites prepared by using organosols of metal sulfides. *Chem. Mater.* **1992**, *4*, 570–576. [[CrossRef](#)]
15. Kassim, A.N.; Min, H.S.; Siang, L.K.; Nagalingam, S.A. SEM, EDAX and UV-Visible studies on the properties of  $Cu_2S$  thin films. *Chalcogenide Lett.* **2011**, *8*, 405–410.
16. Li, H.; Wang, Y.; Jiang, J.; Zhang, Y.; Peng, Y.; Zhao, J.  $CuS$  Microspheres as High-Performance Anode Material for Na-ion Batteries. *Electrochimica Acta* **2017**, *247*, 851–859. [[CrossRef](#)]
17. Liu, Y.; Zhou, Z.; Zhang, S.; Luo, W.; Zhang, G. Controllable synthesis of  $CuS$  hollow microflowers hierarchical structures for asymmetric supercapacitors. *Appl. Surf. Sci.* **2018**, *442*, 711–719. [[CrossRef](#)]
18. Guo, K.; Chen, X.; Han, J.; Liu, Z. Synthesis of  $ZnO/Cu_2S$  core/shell nanorods and their enhanced photoelectric performance. *J. Sol-Gel Sci. Technol.* **2014**, *72*, 92–99. [[CrossRef](#)]
19. Ismail, R.A.; Al-Samarai, A.-M.E.; Muhammed, A.M. High-performance nanostructured p- $Cu_2S$ /n-Si photodetector prepared by chemical bath deposition technique. *J. Mater. Sci. Mater. Electron.* **2019**, *30*, 11807–11818. [[CrossRef](#)]
20. Zhan, Y.; Shao, Z.; Jiang, T.; Ye, J.; Wu, X.; Zhang, B.; Ding, K.; Wu, D.; Jie, J. Cation exchange synthesis of two-dimensional vertical  $Cu_2S/CdS$  heterojunctions for photovoltaic device applications. *J. Mater. Chem. A* **2019**, *8*, 789–796. [[CrossRef](#)]
21. Ramya, M.; Ganesan, S. Study of thickness dependent characteristics of  $Cu_2S$  thin film for various applications. *Iran. J. Mater. Sci. Eng.* **2011**, *8*, 34–40.
22. Podder, J.; Kobayashi, R.; Ichimura, M. Photochemical deposition of  $Cu_xS$  thin films from aqueous solutions. *Thin Solid Films* **2004**, *472*, 71–75. [[CrossRef](#)]
23. Aniefuna, N.K.; Ezenwaka, L.; Umeokwonna, N. Effect of deposition time on the optical properties of Copper Sulphide thin films fabricated by chemical bath deposition method. In *Proceedings of the 1st African International Conference/Workshop on Applications of Nanotechnology to Energy, Health and Environment*, Enugu, Nigeria, 23–29 March 2014; pp. 275–279.
24. Ismail, R.A.; Al-Samarai, A.E.; Ali, A.M.M. Effect of molar concentration of  $CuCl_2$  on the characteristics of  $Cu_2S$  film. *Opt. Quantum Electron.* **2020**, *52*, 1–14. [[CrossRef](#)]
25. He, Y.; Polity, A.; Österreicher, I.; Pfisterer, D.; Gregor, R.; Meyer, B.; Hardt, M. Hall effect and surface characterization of  $Cu_2S$  and  $CuS$  films deposited by RF reactive sputtering. *Phys. B Condens. Matter* **2001**, *308*, 1069–1073. [[CrossRef](#)]
26. Kosoljtkul, P.; Rakkroekong, P.; Vas-Umnuay, P. Parameter-controllable microchannel reactor for enhanced deposition of copper sulfide thin films. *Thin Solid Films* **2018**, *646*, 150–157. [[CrossRef](#)]
27. Su, Y.-W.; Paul, B.K.; Chang, C.-H. Investigation of  $CdS$  nanoparticles formation and deposition by the continuous flow microreactor. *Appl. Surf. Sci.* **2019**, *472*, 158–164. [[CrossRef](#)]
28. Isac, L.A.; Duta, A.; Kriza, A.; Nanu, M.; Schoonman, J. Crystal order in  $Cu_2S$  thin films obtained by spray pyrolysis. *J. Optoelectron. Adv. Mater.* **2007**, *9*, 1265–1268.

29. Nho, P.V.; Ngan, P.H.; Tien, N.Q.; Viet, H.D. Preparation and characterization of low resistivity CuS films using spray pyrolysis. *Chalcogenide Lett.* **2012**, *9*, 397–402.
30. Zhuge, F.; Li, X.; Gao, X.; Gan, X.; Zhou, F. Synthesis of stable amorphous Cu<sub>2</sub>S thin film by successive ion layer adsorption and reaction method. *Mater. Lett.* **2009**, *63*, 652–654. [[CrossRef](#)]
31. Pathan, H.; Desai, J.; Lokhande, C. Modified chemical deposition and physico-chemical properties of copper sulphide (Cu<sub>2</sub>S) thin films. *Appl. Surf. Sci.* **2002**, *202*, 47–56. [[CrossRef](#)]
32. Omwoyo, J.G. *Characterization of Cu<sub>2</sub>S/SnO<sub>2</sub>: F pn Junction for Solar Cell Applications*; Kenyatta University: Nairobi, Kenya, 2019.
33. Gashaw Hone, F.; Abza, T. Short Review of Factors Affecting Chemical Bath Deposition Method for Metal Chalcogenide Thin Films. *Int. J. Thin Film. Sci. Technol.* **2019**, *8*, 3.
34. Allouche, N.K.; Ben Nasr, T.; Guasch, C.; Turki, N.K. Optimization of the synthesis and characterizations of chemical bath deposited Cu<sub>2</sub>S thin films. *Comptes Rendus. Chim.* **2010**, *13*, 1364–1369. [[CrossRef](#)]
35. Hone, F.G.; Dejene, F.B. Cationic concentration and pH effect on the structural, morphological and optical band gap of chemically synthesized lead sulfide thin films. *J. Mater. Res. Technol.* **2019**, *8*, 467–474. [[CrossRef](#)]
36. Kırmızıgül, F.; Güneri, E.; Gümüş, C. Effects of different deposition conditions on the properties of Cu<sub>2</sub>S thin films. *Philos. Mag.* **2013**, *93*, 511–523. [[CrossRef](#)]
37. Patil, M.; Sharma, D.; Dive, A.; Mahajan, S.; Sharma, R. Study of various synthesis techniques of nanomaterials. In *AIP Conference Proceedings*; AIP Publishing LLC: Melville, NY, USA, 2018.
38. Chopra, K.L. *Thin Film Phenomena*; McGraw-Hill: New York, NY, USA, 1969.
39. Khalil, M.H.; Mohammed, R.Y.; Ibrahim, M.A. The Influence of CBD Parameters on the Energy Gap of ZnS Narcissus-Like Nanostructured Thin Films. *Coatings* **2021**, *11*, 1131. [[CrossRef](#)]
40. Makuła, P.; Pacia, M.; Macyk, W. Investigation of optical properties of the PbS/CdS thin films by thermal Evaporation. *J. Electron Devices* **2012**, *12*, 761–766.
41. Makuła, P.; Pacia, M.; Macyk, W. *How to Correctly Determine the Band Gap Energy of Modified Semiconductor Photocatalysts Based on UV-Vis Spectra*; ACS Publications: Washington, DC, USA, 2018.
42. Mohammed, K.A.; Ahmed, S.M.; Mohammed, R.Y.; Mohammed, K. Investigation of Structure, Optical, and Electrical Properties of CuS Thin Films by CBD Technique. *Crystals* **2020**, *10*, 684. [[CrossRef](#)]
43. Shinde, M.S.; Ahirrao, P.B.; Patil, I.J.; Patil, R.S. *Thickness Dependent Electrical and Optical Properties of Nanocrystalline Copper Sulphide Thin Films Grown by Simple Chemical Route*; NISCAIR-CSIR: New Delhi, India, 2012.
44. Ouachtari, F.; Rmili, A.; Elidrissi, B.; Bouaoud, A.; Erguig, H.; Elies, P. Influence of Bath Temperature, Deposition Time and S/Cd Ratio on the Structure, Surface Morphology, Chemical Composition and Optical Properties of CdS Thin Films Elaborated by Chemical Bath Deposition. *J. Mod. Phys.* **2011**, *02*, 1073–1082. [[CrossRef](#)]
45. Sangamesha, M.; Pushapalatha, K.; Shekar, G. Effect of concentration on structural and optical properties of CuS thin films. *Int. J. Pure Appl. Res. Eng. Technol.* **2013**, *2*, 227.
46. Vas-Umnuay, P.; Chang, C.-H. Growth Kinetics of Copper Sulfide Thin Films by Chemical Bath Deposition. *ECS J. Solid State Sci. Technol.* **2013**, *2*, P120–P129. [[CrossRef](#)]
47. Manjulavalli, T.; Kannan, A. Effects of deposition time on structural, optical and electrical properties of chemically deposited Cu<sub>2</sub>S thin films. *J. Chem. Tech. Res.* **2015**, *8*, 607–616.
48. Xu, H.; Dong, J.; Chen, C. One-step chemical bath deposition and photocatalytic activity of Cu<sub>2</sub>O thin films with orientation and size controlled by a chelating agent. *Mater. Chem. Phys.* **2014**, *143*, 713–719. [[CrossRef](#)]
49. Yu, M.; Draskovic, T.I.; Wu, Y. Understanding the crystallization mechanism of delafossite CuGaO<sub>2</sub> for controlled hydrothermal synthesis of nanoparticles and nanoplates. *Inorg. Chem.* **2014**, *53*, 5845–5851. [[CrossRef](#)] [[PubMed](#)]
50. Rondiya, S.; Rokade, A.; Gabhale, B.; Pandharkar, S.; Chaudhari, M.; Date, A.; Chaudhary, M.; Pathan, H.; Jadkar, S. Effect of Bath Temperature on Optical and Morphology Properties of CdS Thin Films Grown by Chemical Bath Deposition. *Energy Procedia* **2017**, *110*, 202–209. [[CrossRef](#)]
51. Ahmed, H.S.; Mohammed, R.Y.; Khalil, M.H. Effects of Deposition Time And PH on The Characterization of Chemically Synthesized Composite Nano-Wires of Cu<sub>2</sub>S Thin Films. *Sci. J. Univ. Zakho* **2021**, *9*, 184–192. [[CrossRef](#)]
52. Muhammed, A.M.; Ibrahim, A.E.; Ismail, R.A. Study an Effect of Thiourea Concentration on the Structural, Optical and Electrical Properties of (Cu<sub>2</sub>S) film Prepared by Chemical Bath Deposition (CBD). *Kirkuk Univ. J.-Sci. Stud.* **2019**, *14*, 97–115. [[CrossRef](#)]